Probing the local environment of substitutional Al3+ in goethite using X-ray absorption spectroscopy and first-principles calculations

Manoj Ducher, Marc Blanchard, Delphine Vantelon, Ruidy Nemausat, Delphine Cabaret

Probing the local environment of substitutional Al^{3+} in goethite using X-ray absorption spectroscopy and first-principles calculations

Manoj, Ducher[1] & Marc, Blanchard[1] & Delphine, Vantelon[2] & Ruidy, Nemausat[1] & Delphine Cabaret[1]

[1]Institut de Minéralogie, de Physique des Matériaux et de Cosmochimie (IMPMC),
Sorbonne Universités, UPMC Univ Paris 06, CNRS UMR 7590,
Muséum National d'Histoire Naturelle, IRD UMR 206,
4 place Jussieu, F-75005 Paris, France
Tel.: +33-(0)1-44279832
Fax: +33-(0)1-44273785
manoj.ducher@impmc.upmc.fr

[2]Synchrotron SOLEIL, L'Orme des Merisiers, 91192 Gif-sur-Yvette Cedex, France.

Abstract

We present experimental and calculated Al K-edge X-ray absorption near-edge structure (XANES) spectra of aluminous goethite with 10 to 33 mol % of AlOOH and diaspore. Significant changes are observed experimentally in the near and pre-edge regions with increasing Al concentration in goethite. First-principles calculations based on density-functional theory (DFT) reproduce successfully the experimental trends. This permit to identify the electronic and structural parameters controlling the spectral features and to improve our knowledge of the local environment of Al^{3+} in the goethite-diaspore partial solid solution.

In the near-edge region, the larger peak spacing in diaspore compared to Al-bearing goethite is related to the nature (Fe or Al) of the first cation neighbours around the absorbing Al atom (Al). The intensity ratio of the two near-edge peaks, which decreases with Al concentration, is correlated with the average distance of the first cations around Al* and the distortion of the AlO_6 octahedron. Finally, the decrease in intensity of the pre-edge features with increasing Al concentration is due to the smaller number of Fe atoms in the local environment of Al since Al atoms tend to cluster. In addition, it is found that the pre-edge features of the Al K-edge XANES spectra enable to probe indirectly empty 3d states of Fe. Energetic, structural and spectroscopic results suggest that for Al concentrations around 10 mol %, Al atoms can be considered as isolated whereas above 25 mol %, Al clusters are more likely to occur.*

1 Introduction

Goethite (α-FeOOH) is a very common iron oxyhydroxide mineral of soils and sediments. Goethite is also one of the most stable Fe(III) oxide along with hematite. The high specific surface area of this mineral gives it the ability to control the mobility of metals and nutrients through adsorption and incorporation mechanisms (Trivedi et al, 2001; Kaur et al, 2009). Even if many elements can be incorporated through the replacement of iron atoms into the goethite structure, aluminium is the most common chemical impurity. Cornell and Schwertmann (2003) state that the Al for Fe substitution is possible up to 33 mol %. At the other end of the partial solid solution, the aluminous end-member is diaspore (α-AlOOH). The presence of aluminium in goethite leads to structural modifications of bond lengths and lattice parameters, due to the smaller ionic radius of Al compared to Fe (Schulze, 1984; Blanch et al, 2008). These structural differences observed in Al-substituted goethite are associated with modifications of the surface and magnetic properties, the thermal stability and the dissolution rate of this

mineral (e.g., Fleisch et al, 1980; Murad and Schwertmann, 1983; Schwertmann, 1984; Schulze and Schwertmann, 1987; Liu et al, 2006; Fritsch et al, 2005; Wells et al, 2006).

The local structure of aluminous goethites has been studied using various experimental and theoretical approaches (Ildefonse et al, 1998; Alvarez et al, 2007; Bazilevskaya et al, 2011; Blanchard et al, 2014; Kim et al, 2015). By performing solid-state nuclear magnetic resonance experiments (NMR), Kim et al (2015) show that the use of static ^{27}Al spin echo mapping provides clear evidence of Al incorporation into the goethite structural framework. Alvarez et al (2007) investigate the local structure of (Al,Mn)-substituted goethites using XANES at the Al, Fe and Mn *K*-edges and EXAFS (extended X-ray absorption fine structure) at the Mn and Fe *K*-edges. The Al *K*-edge XANES spectra confirm the octahedral coordination of Al, but the spectral modifications observed when the Al/Mn ratio varies are not further interpreted. Using first-principles calculations based on DFT, Blanchard et al (2014) specify that the Al for Fe substitution in the goethite structure (6.35 mol % and 12.5 mol % of AlOOH) leads to a local and nearly full structural relaxation. In addition, Blanchard et al (2014) show that the DFT modelling of infrared spectra permit to separate the effect of Al substitution from that of structural defects, non-stoichiometric hydroxyl incorporation or particle shape. From a fingerprint analysis of XANES spectra of aluminous goethites (10 to 33 mol % of AlOOH), Ildefonse et al (1998) propose gibbsite-like and diaspore-like Al distributions at low and high Al concentrations, respectively. On the contrary, using DFT calculations, Bazilevskaya et al (2011) find that a diaspore-like clustered distribution of Al atoms is energetically favoured whatever the Al concentration. From these studies, it appears that the local environment of substituted Al in goethite remains quite unclear and deserves further investigation.

Local structure probes, such as NMR or X-ray absorption spectroscopy, when combined with first-principles calculations, are the techniques of choice to study structural modifications induced by point defects or dopants in solids (Farnan et al, 2003; Mitchell et al, 2011; Gaudry et al, 2005, 2007). Here we present an experimental and theoretical study of Al *K*-edge XANES spectra in diaspore and aluminous goethites. Al *K*-edge experiments are conducted on aluminous goethites with AlOOH concentrations ranging from 10 mol % to 33 mol %. DFT calculations are performed using the same concentrations and Al structural arrangements as those studied by Bazilevskaya et al (2011). The spectral differences between aluminous goethite and diaspore, on the one hand, and within the aluminous goethite series, on the other hand, are clearly identified and explained. Particuliar attention is paid on the Al *K* pre-edge region, which turns out to be a probe of the 3*d* states of neighbouring Fe.

2 Methodology

2.1 Samples and experimental Al *K*-edge XANES

Four aluminous goethite and one diaspore powder samples are studied here. The series of aluminous goethite was synthesised and studied by Goodman and Lewis (1981). The Al concentrations are 10, 15, 25 and 33 mol % of AlOOH. The diaspore sample is the same used by Ildefonse et al (1998). Al-bearing goethite and diaspore samples are prepared by crushing the powders on indium foils.

Al *K*-edge XANES measurements are performed at the LUCIA beamline (Flank et al, 2006) at synchrotron SOLEIL. The synchrotron ring is operated at 2.75 GeV in multibunch mode with top-up injection, the total current of the beam is 430 mA. The X-ray source is an APPLE-II undulator and two $KTiOPO_4$ (011) single crystals are used as monochromator. The fluorescence emission is detected by a mono-element energy dispersive drift diode in four channels. To avoid as much as possible self-absorption, the detection angle is set at nearly 0° during all the measurements. The data are normalised and corrected for self-absorption, as described by Manuel et al (2012). A step of 0.05 eV is used to acquire the spectra in the region 1560-1580 eV.

2.2 Aluminous goethite and diaspore models

Goethite (α-FeOOH) and diaspore (α-AlOOH) both have an orthorhombic unit cell that are described, here, in the *Pnma* space group. The unit cell contains four formula units (16 atoms). Goethite is antiferromagnetic; half of the Fe atoms have their spin up density of states larger than their spin down density of states and *vice versa* for the other half. Spins

up and spin down cations are found in alternate chains of octahedra that run along the *b*-axis (Cornell and Schwertmann, 2003).

All calculations are performed using a 1×3×2 supercell, which initially contains 24 Fe, 48 O and 24 H. This size of supercell leads to almost equivalent *a*, *b* and *c* lattice parameters ($\sim$ 9 Å) and is found large enough for XANES calculations, since it avoids the interaction of the atom having a core hole with its periodic images. Models of Al-bearing goethite are based on those investigated by Bazilevskaya et al (2011). The isomorphous Al for Fe substitutions are made in such a way to preserve the antiferromagnetic ordering. Two concentrations, 8.3 and 25 mol % of AlOOH, are modelled and correspond to two and six Al for Fe substitutions in the supercell, respectively. For each concentration, two configurations called "cluster" and "isolated" are built as presented in Fig. 1 and correspond to two different Al distribution in the supercell. The distinction between cluster and isolated models resides in the Al-Al distances that are short ($\simeq$ 3.5 Å) in the former and large ($>$ 5 Å) in the latter. In a similar way, a 1×3×2 (*Pnma*) diaspore supercell is built. The XANES spectra are calculated for these four aluminous goethite models and for diaspore.

2.3 Computational details

Structural relaxations and self-consistent field (SCF) calculations are done with the PWscf code based on DFT, plane-waves and pseudopotentials (Giannozzi et al, 2009) and XANES calculations with the XSpectra code (Gougoussis et al, 2009; Taillefumier et al, 2002), both included in the Quantum Espresso suite of codes. We use spin-polarised generalised gradient approximation (GGA) functionals with the Perdew-Burke-Ernzerhof (PBE) parameterisation (Perdew et al, 1996), and ultrasoft Vanderbilt-type GIPAW pseudopotentials. The Al ultrasoft pseudopotential is generated considering the 3*s*, 3*p* and 3*d* states as valence states, with cut-off radii of 2.10, 2.10 and 1.90 a_0, respectively; the *d* states being the local part (a_0 is the Bohr radius). The pseudopotential of the absorbing Al atom (Al*) is generated from the Al electronic configuration with a single 1*s* electron. The valence states of the O ultrasoft pseudopotential are the 2*s*, 2*p*, 3*d* states, with cut-off radii of 1.35, 1.35 and 1.30 a_0 and the *d* states are the local part. Fe and H ionic cores are described by ultrasoft pseudopotentials from the GBRV library (Garrity et al, 2014). The cut-off energies for wavefunctions and charge-density are determined from convergence tests and set to 60 Ry and 720 Ry, respectively. The electronic occupations are smeared with a Gaussian spreading of 0.007 Ry.

For each model (Fig. 1), a relaxation calculation is performed during which lattice parameters, atomic positions and magnetic moments are all free to relax. The convergence threshold on the total energy for self-consistency is set at 10^{-9} Ry, total energy between two consecutive SCF steps at 10^{-4} Ry and forces at 10^{-3} Ry$/a_0$. Following the structural relaxation, SCF calculations are made with the 1*s* core hole successively located on each Al* of the supercell. Due to the 1*s* core hole, the total charge of the supercell is set to $+1$ (full core hole approach). For all SCF calculations (with or without the core-hole) a shifted 2×2×2 *k*-points grid according to the scheme of Monkhorst and Pack (1976) is found to be satisfactory.

Thereupon, theoretical individual spectra are calculated in the electric-dipole approximation, on a 3×3×3 *k*-points grid and with a constant broadening parameter of 0.7 eV. The individual spectra correspond to the Al atoms separately considered as the absorbing atom, within the supercell associated to a given model. These individual spectra result from the average of three absorption cross-sections successively performed for the X-ray polarisation vector along [100], [010] and [001] directions of the supercell. Then, for each model, the individual spectra are averaged by taking into account the core-level shift as explained by Lelong et al (2014). The calculated XANES spectra are then aligned with the experimental ones with respect to the energy position of the main XANES peak. Finally, in order to interpret the pre-edge features, partial electronic densities of states (DOS) are calculated on the systems having the core hole, using Löwdin projections, 3×3×3 Monkhorst-Pack *k*-points grid and a Gaussian broadening of 0.02 eV.

3 Results

3.1 Al *K*-edge XANES spectra of aluminous goethite and diaspore

Experimental Al *K*-edge XANES spectra of diaspore and aluminous goethite are presented in Fig. 2a. The aluminous goethite spectra show two main peaks, A and B, at 1568.8 eV and 1572.0 eV respectively, and pre-edge features around 1563 eV. Di-

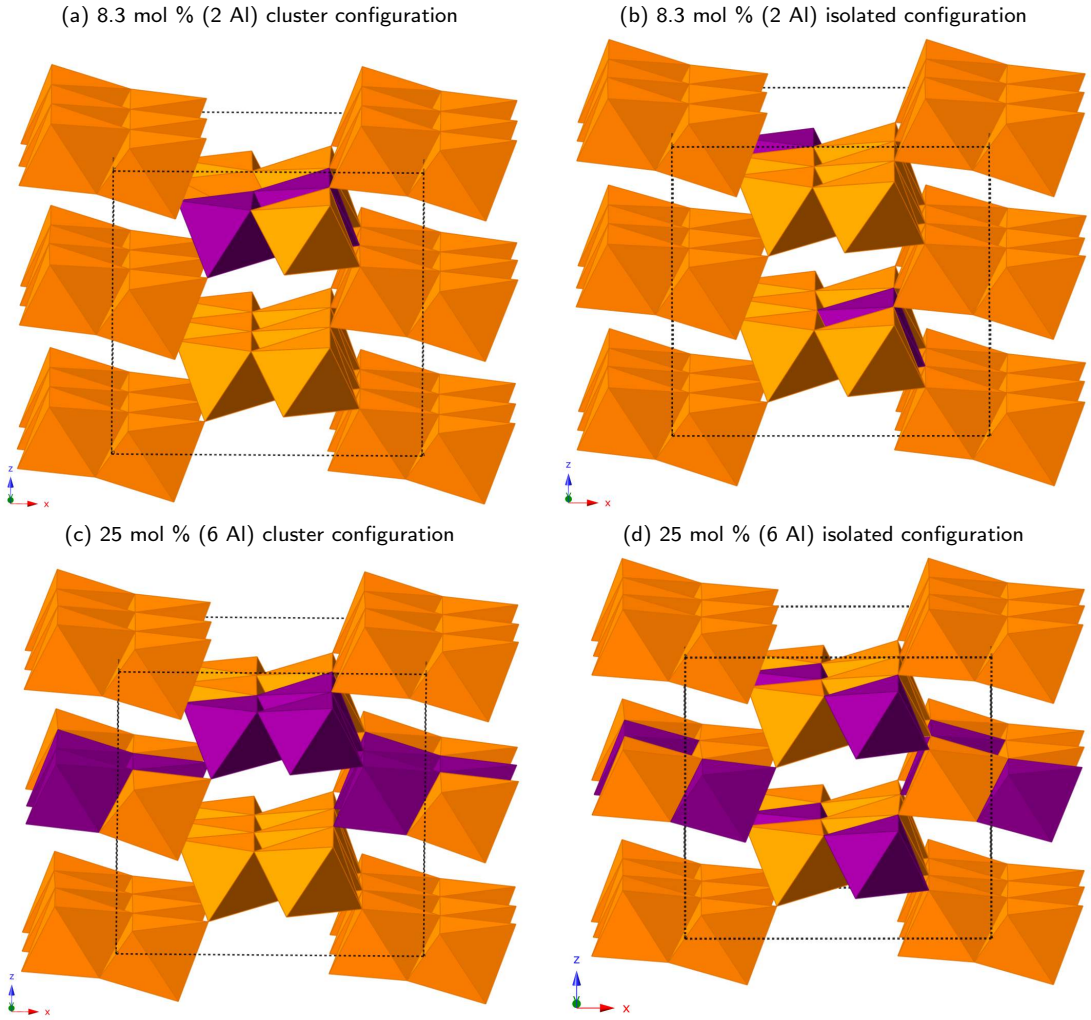

Figure 1: *Polyhedral representation (after structural relaxation) of the four aluminous goethite 1×3×2 supercells considered in the present study: low Al concentration (a and b), high Al concentration (c and d). The cluster (a and c) and isolated (b and d) configurations are defined relative to the Al-Al distances, which are* $\simeq 3.5\mathring{A}$ *and* $> 5\mathring{A}$*, respectively.*

aspore also displays two peaks at 1568.5 eV and 1572.5 eV. The A-B peak spacing is thus larger in diaspore (4 eV) than in Al-bearing goethite (3.2 eV). It can be seen that as the Al concentration increases, the intensity of both peaks decreases monotonically and more specifically, the B/A ratio (i.e., intensity ratio of both peaks) decreases. The B/A ratio at 10 mol % of AlOOH is 15 % higher than the ratio in diaspore, and decreases to 8 % at 33 mol % of AlOOH. Finally, the pre-edge region strongly differs between diaspore and the aluminous goethite series. The XANES spectrum of diaspore exhibits quite an intense pre-edge feature at 1565.8 eV (labelled P), while the aluminous goethites pre-edges are made of two peaks (labelled P_1 and P_2) located at lower energies (1562.0 eV and 1563.5 eV). The intensity of P_1 and P_2 decreases with increasing Al concentration (inset of Fig. 2a). Our XANES spectra, measured in total fluorescence yield, are in overall agreement with those recorded by Ildefonse et al (1998) on the same aluminous goethite samples, using total electron yield detection. Both series of spectra exhibit the same trends except in the pre-edge region, which was not well defined in the measurements of Ildefonse et al (1998) due to a lack of resolution.

The four calculated spectra for the cluster and isolated configurations at 8.3 and 25 mol % of AlOOH are plotted in Fig. 2b, along with the calculated spectrum of diaspore. The two main peaks A and B, seen in experimental spectra, are also visible here. First, the theoretical A-B peak spacing

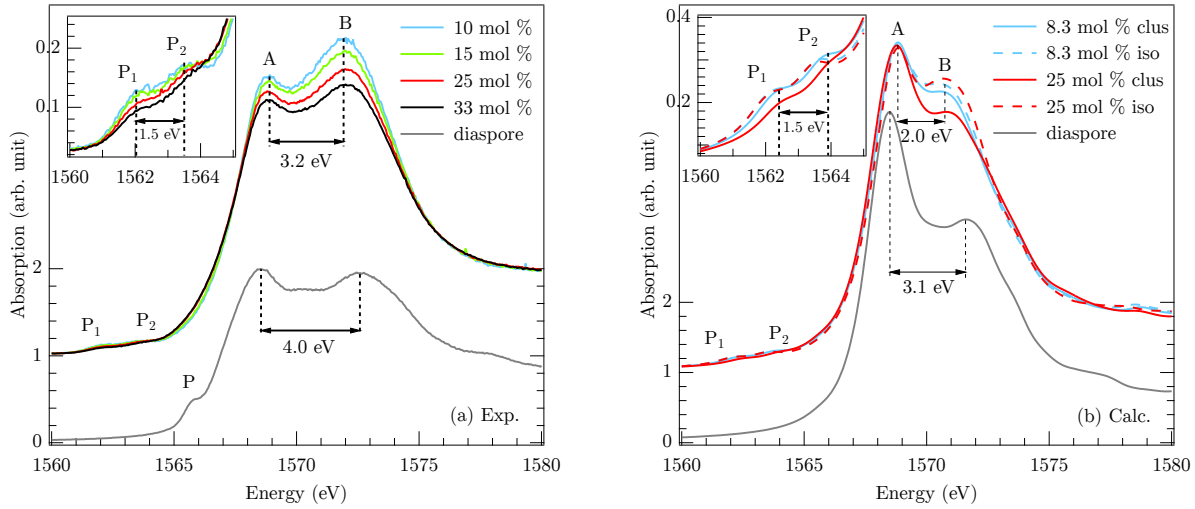

Figure 2: *Experimental (a) and calculated (b) Al K-edge XANES spectra of aluminous goethite and diaspore. Inset: zoom on the pre-edge region of the aluminous goethite XANES spectra.*

is smaller in aluminous goethite ($\sim$ 2.0 eV) than in diaspore ($\sim$ 3.1 eV) as observed experimentally. Second, the peak intensities change between the two concentrations, but also between the cluster and isolated configurations. The larger decrease in intensity of peak B compared to peak A (i.e., the B/A ratio decrease with increasing Al concentration) is successfully reproduced, only if the 25 mol % isolated configuration is ruled out. Compared to diaspore, the B/A ratio at 8.3 mol % of AlOOH is larger by 26 % (resp. 30 %) for the isolated (resp. cluster) model, and decreases to 18 % for the cluster model at 25 mol % of AlOOH. Finally, while the pre-edge peak P of diaspore is not reproduced by the calculation, the pre-edge region of all aluminous goethites exhibits two peaks, P_1 and P_2, in good agreement with experiment. If we again rule out the 25 mol % isolated configuration, the P_1 and P_2 intensities decrease with increasing Al concentration, as experimentally observed.

For the whole series (diaspore included), two main discrepancies appear when comparing experiment with calculation: (i) theoretical A-B peak spacings are smaller than experimental ones, (ii) calculations overestimate the intensity of peak A. The smaller calculated A-B peak spacing is connected to the usual underestimation of the band-gap in GGA that also gives, in the present case, lower $1s \rightarrow p$ transition energies. Such a contraction of the XANES features as modelled within DFT is often observed (Cabaret et al, 2005; Trcera et al, 2009) and could be corrected by performing additional *GW* self-energy calculation using a many-pole model (Kas et al, 2007, 2009). The discrepancy related to the overestimation of the peak A intensity was already observed at the Al *K*-edge in previous simulations using the same theoretical approach (Cabaret et al, 2005; Cabaret and Brouder, 2009; Manuel et al, 2012). It was attributed to the overestimation of the attraction potential created by the 1*s* core-hole in the full core-hole approach. Thus, these technical disagreements are inherent to DFT-GGA. They are well understood and do not hamper the XANES DFT analysis presented in the next section.

3.2 Relative energies and structural properties of aluminous goethite models

After structural relaxation, the total energies of the aluminous goethite models show that at the 25 mol %, the isolated configuration has an energy 169 meV greater than the cluster one. This energy difference supports the fact that the former model is not consistent with the observed spectral trends. At 8.3 mol %, the total energy difference (33 meV) is in favour of the isolated model while the theoretical XANES spectra are not able to discriminate between the two Al distributions.

Table 1: *Local environment of Al (resp. Fe) in the four aluminous goethite models and diaspore (resp. goethite): average M-O and M-OH bond lengths with M=Al (resp. Fe), average M-M′ interatomic distance with M′ being the first cation neighbours. The theoretical unit cell volume is given and compared with experimental values. Experimental volumes are obtained considering a linear evolution (Vegard's law) between goethite and diaspore. The interatomic distances and cell volumes of the most energetically favourable structural models are in bold.*

	Coordination shell		First cation neighbours shell		Cell volume (Å^3)	
	⟨M-O⟩ (Å)	⟨M-OH⟩ (Å)	⟨M-M′⟩ (Å)	M′ nature and number	Calc.	Exp.
goethite	1.95	2.13	3.32	8 Fe	141.05	138.58[a]
8.3 mol % cluster/isolated	1.91/**1.92**	1.98/**1.96**	3.29/**3.28**	1 Al, 7 Fe / 8 Fe	139.36/**139.33**	136.85
25 mol % cluster/isolated	**1.90**/1.92	**1.99**/1.95	**3.25**/3.29	3.33 Al, 4.67 Fe / 8 Fe	**136.21**/136.47	133.37
diaspore	1.88	1.99	3.16	8 Al	118.02	117.75[a]

[a](Blanch et al, 2008)

The relaxation also leads to structural modifications in aluminous goethite models. As shown by the calculations, the spectral features evolve with both Al concentration and Al distribution. Thus the structural relaxation around the Al* atom in the four aluminous goethite models has to be investigated in detail. Since XANES is sensitive to the first few atomic shells around the absorbing atom, the structural analysis is focused here on the local atomic arrangement up to the first cation neighbours of Al. Table 1 gives the average distances between Al and its first surrounding atomic shells (Al-O, Al-OH and Al-Al/Fe) in the Al-substituted goethite models and in diaspore. For comparison, the corresponding Fe-O, Fe-OH and Fe-Fe average distances in goethite are also indicated. In the four aluminous goethite models, the average bond lengths within the AlO_6 octahedra overall tend to be those of diaspore. In addition, the Al-O and Al-OH average bond lengths indicate that the AlO_6 octahedron is more regular for the isolated configurations than for the cluster ones. Beyond the Al coordination sphere, the first cation neighbours shell is composed of eight atoms, the nature of which depends on the aluminous goethite model (Table 1). For instance, in the cluster Al distribution, the number of Fe cation neighbours logically decreases with increasing Al concentration. The average Al-(Al,Fe) distances in the Al-substituted goethite models are between the average Fe-Fe distance in goethite and the average Al-Al distance in diaspore. Specifically, the average cation-cation distance ⟨M-M′⟩ decreases with increasing Al concentration. To go further into the structural model analysis, the distortion of the AlO_6 octahedra is quantitatively investigated as a function of Al concentration by two parameters (Fig. 3): the bond length deviation and the bond angle variance (Fleet, 1976; Robinson et al, 1971).

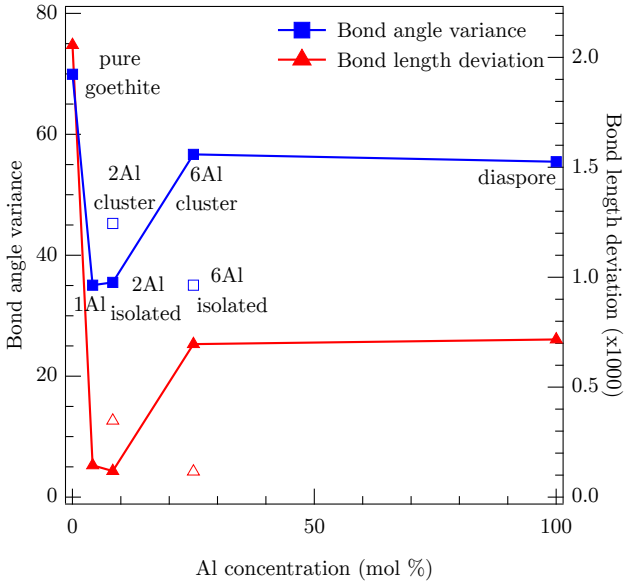

Figure 3: *Bond angle variance and bond length deviation of $FeO_3(OH)_3$ octahedra in goethite, $AlO_3(OH)_3$ octahedra in aluminous goethite and diaspore as a function of Al concentration. 1Al, 2Al, 6Al correspond to the number of Fe-Al substitutions present in the simulation cell. The most energetically favourable models (full symbols) are connected between them by a solid line.*

The bond length deviation is defined as:

$$\Delta = \frac{1}{6}\sum_{i=1}^{6}\left[\frac{(l_i - \bar{l})}{\bar{l}}\right]^2, \qquad (1)$$

where l_i is one of the six bond lengths of the octahedron and $\bar{l}$ is the average bond length. The bond angle variance is defined as:

$$\sigma^2 = \frac{1}{11}\sum_{i=1}^{12}(\theta_i - 90^\circ)^2, \qquad (2)$$

where θ_i is one of the twelve bond angles of the octahedron. Δ and σ^2 are calculated for each Al site (Fe sites in goethite) and averaged thereafter. Starting

from the structure of pure goethite, the substitution of one Fe with one Al (noted 1Al) makes the AlO_6 octahedron more regular than in both goethite and diaspore. If a second Al substitutes for a Fe far from the first Al (isolated configuration), the octahedra are as regular as in the 1Al case. On the contrary, if the two Al are clustered, the distortion increases. The fact that the distortion is more important in the cluster configuration than in the isolated one is also observed at 25 mol % of AlOOH (i.e., 6Al models). At 25 mol %, in a clustered distribution of Al, the AlO_6 octahedra is more distorted than at 8.3 mol % and resemble to that found in diaspore.

4 Discussion

4.1 Origin of the spectral evolution in the near-edge region

Ildefonse et al (1998) suggested that the electronic modifications occurring during the Al for Fe substitution could be at the origin of the spectral differences in the near-edge region (first 10 eV). We show here that electronic modifications, such as the substitution of high spin Fe^{3+} with consequences on the local magnetic moments, account for the A-B peak spacing difference, on the one hand, and induce structural differences that explain the B/A ratio decrease, on the other hand.

Table 2: *Nature of the cations present in the four fictitious models used to investigate the A-B peak spacing difference between aluminous goethite series and diaspore. These models were built keeping the crystallographic structure of diaspore (here "diasp 24 Al") and changing only the nature of the cations.*

model	1st cation neighbours around the absorbing Al*	others
diasp 24 Al	8Al	15Al
diasp 9Al + 15Fe	8Al	15Fe
diasp 7Al + 17Fe	6Al + 2Fe	15Fe
diasp 5Al + 19Fe	4Al + 4Fe	15Fe
diasp 1Al + 23Fe	8Fe	15Fe

As seen previously, the Al/Fe ratio around Al* changes with concentration and with the Al distribution. In order to investigate the influence of the nature of the cation neighbours on the spectra, we build four fictitious models starting from the structure of diaspore. In these models, each Al* is surrounded by eight cation neighbours with various Al/Fe ratios (Table 2). The crystallographic structure is kept fixed, i.e., all interatomic distances and cell parameters are those of diaspore, only the chemical composition changes. The calculated spectra of these models are plotted in Fig. 4. The peak spacing is equal in both the models where Al* is surrounded by eight Al (diasp 24 Al and diasp 9 Al + 15 Fe). As the number of Al cation neighbours decreases, the peak spacing decreases. These observations clearly suggest that the electronic modifications due to the nature of the cation neighbours, have an impact on the peak spacing: the more the Al atoms are present around Al*, the larger the peak spacing. None of our relaxed aluminous goethite models has an Al* site completely surrounded by Al (Table 1). This explains the similar peak spacing within the aluminous goethite series and the shorter peak spacing for aluminous goethites compared to diaspore, observed both experimentally and theoretically.

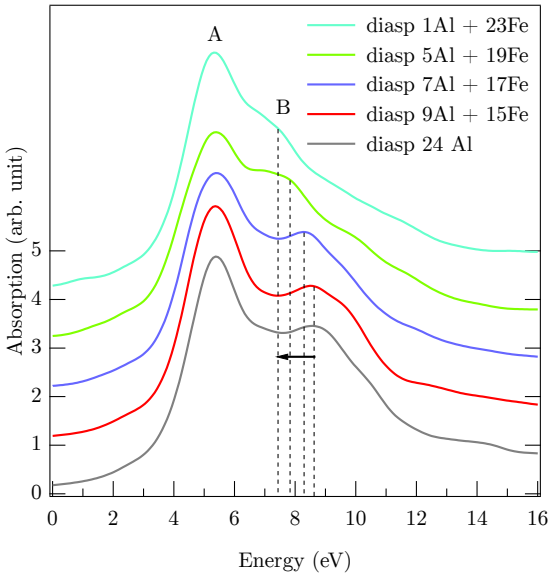

Figure 4: *Theoretical Al K-edge XANES spectra of the structural models described in Table 2, i.e., diaspore and four fictitious models built from the diaspore structure. The A-B spacing is controlled by the nature of the cation neighbours around the absorbing atom: as the Al/Fe ratio decreases among the first cation neighbours, the A-B peak spacing decreases (left arrow). The origin of the energy scale for the absorption cross-section is set to be the highest occupied band energy given by the SCF calculation of the supercells including the core-hole.*

The variation of the A-B peak intensities with Al concentration is the second main effect to be investigated. Experimentally, the intensities change greatly between aluminous goethite and diaspore: the intensity of peak A in the goethite series is around 50% higher than that in diaspore. To a lesser extent, within the aluminous goethite series, the in-

tensities of both peak A and B decrease as the concentration increases from 10 to 33 mol % of AlOOH. It is likely that such effects are related to structural modifications induced by electronic ones: the substitution of Fe by Al, which has a smaller ionic radius. The main structural difference between goethite and diaspore is the shorter interatomic distances in the latter while the angles remain comparable. The observed decrease of the B/A ratio with increasing Al content could be linked with both the average distance between Al* and the first cation neighbours, as this distance decreases with increasing Al concentration (Table 1), and the distortion of Al octahedra, which is related to the Al-O and Al-OH bond lengths (Fig. 3). Indeed, the distortion parameters suggest that as distortion increases, the B/A ratio decreases, resulting in a less intense peak B at high Al concentration. This means that in addition to the cation-cation distance, the distortion of Al octahedra controls the peak intensity. Moreover, it can be seen that at 25 mol % in a cluster arrangement of Al, which is the most favourable configuration, there is locally a diaspore-like structure, as suggested by Ildefonse et al (1998). Indeed, the distortion of AlO_6 octahedra is very close to that in diaspore (see Fig. 3).

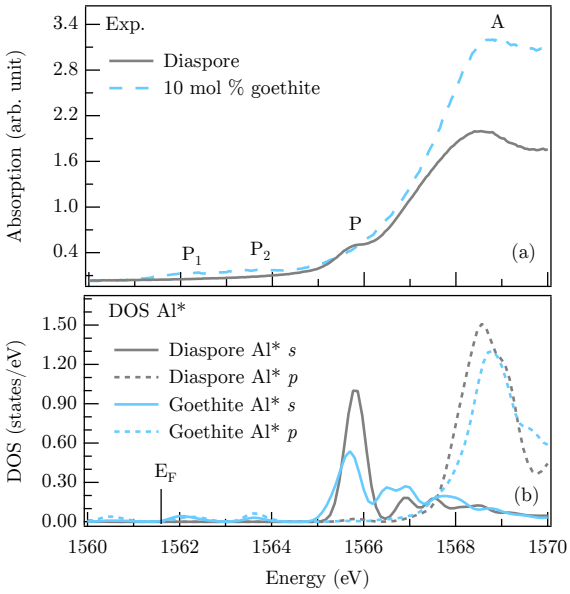

Figure 5: *(a) Experimental Al K-edge XANES spectra of diaspore and aluminous goethite. (b) Corresponding calculated 3s and p DOS projected on Al*. The pre-edge peak P at 1565.8 eV in diaspore is attributed to vibration-induced $1s \rightarrow 3s$ transitions. It is not observed in aluminous goethite spectrum where the localised empty 3s states are almost twice smaller. E_F denotes the Fermi level and the energy scale of the DOS has been shifted in order to match with experimental XANES spectra.*

4.2 Pre-edge analysis

The pre-edge of aluminous goethite exhibits two main peaks, P_1 and P_2, well separated from the edge jump. Moreover, their intensities decrease with increasing Al concentration. These features are well reproduced by our theoretical spectra (Fig. 2). In contrast, the experimental spectrum of diaspore has a pre-edge peak P at 1565.8 eV. To investigate the absence of this peak in aluminous goethite spectra, calculated 3*s* and *p* DOS, projected on Al* in diaspore and aluminous goethite at 8.3 mol % in isolated configuration, are plotted in Fig. 5 along with the corresponding experimental XANES spectra. Localised empty 3*s* states are present at around 1565.8 eV in diaspore and in aluminous goethite. The origin of peak P is attributed to forbidden $1s \rightarrow 3s$ transitions induced by vibrations as shown by Cabaret and Brouder (2009), Brouder et al (2010) and Manuel et al (2012). The intensity of the 3*s* DOS peak in diaspore is 1.9 times larger than in aluminous goethite. Thus, in the case of aluminous goethite, the rate of the vibration-induced $1s \rightarrow 3s$ transitions is too weak to result in a visible peak in the corresponding Al *K*-edge spectrum.

In order to understand the origin of the P_1 and P_2 features, DOS projected on Al*, first O neighbours and first Fe cation neighbours are plotted along with the experimental and calculated pre-edge spectra (Fig. 6). At energies corresponding to P_1 and P_2 positions, the presence of empty *p* states of O and Al*, and empty 3*d* states of Fe is shown by DOS calculations. This allows the assignment of the pre-edge peaks to transitions from 1*s* to empty *p* states of Al*, which are orbitally mixed with the 3*d* states of Fe through the *p* states of the neighbouring oxygen atoms. Previous studies have shown that the empty 3*d* states of Fe can be probed at the Fe *K*-edge in the pre-edge region (Arrio et al, 2000; Wang et al, 2010) and at the O *K*-edge, thanks to the O 2*p* - Fe 3*d* orbital mixing (de Groot et al, 1989; Zhang et al, 2003; Gilbert et al, 2007). This study shows that the 3*d* states of Fe can also be probed indirectly through Al *K*-edge XANES measurements in aluminous goethite. Unlike the Fe 3*d* states probed at the Fe *K* pre-edge, the Fe 3*d* states probed at the Al *K*-edge (and at the O *K*-edge) are not affected by the presence of the core-hole.

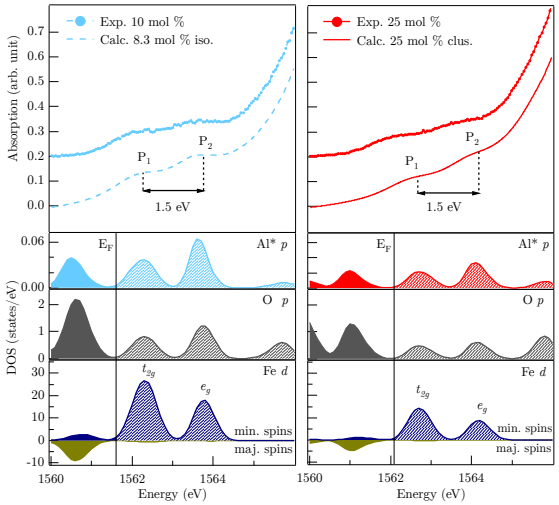

Figure 6: *Experimental (*10 mol % *and* 25 mol %*) and calculated (*8.3 mol % *and* 25 mol %*) pre-edge regions of Al K-edge XANES spectra of aluminous goethite. The corresponding Al* p, the first six O neighbours p and the first Fe neighbours d partial densities of states are plotted. Fe* 3*d DOS are separated into minority and majority spin states. E_F denotes the Fermi level and the energy scale of the DOS has been shifted in order to match with experimental XANES spectra. The smaller number of empty Fe* 3*d states for the* 25 mol % *cluster model than for the* 8.3 mol % *isolated model is explained by a smaller number of Fe atoms around the absorbing Al.*

In goethite and aluminous goethite, each Fe is in high spin trivalent state within an octahedral environment. In the O_h symmetry point group approximation, the Fe 3*d* state are split into t_{2g} and e_g orbitals, with occupied majority-spin states and unoccupied minority-spin states. This description is in total agreement with the DOS calculations shown in Fig. 6. Consequently, peaks P_1 and P_2 are indirect experimental probe of Fe 3*d* t_{2g} and e_g empty orbitals, respectively. The energy separation between P_1 and P_2 is found to be about 1.5 eV, both in experimental and calculated spectra. This value is consistent with (i) ground state DOS calculations performed in pure goethite by Otte et al (2009) and Russell et al (2009), and (ii) the O *K*-edge XANES spectrum of bulk goethite recorded by Gilbert et al (2007). In addition, the P_1-P_2 energy difference may provide an estimate of the Δ_0 crystal field parameter (in O_h symmetry), which is defined as the energy difference between the single-electron configurations ${t_{2g}}^0{e_g}^1$ and ${t_{2g}}^1{e_g}^0$ (König and Kremer, 1977). The crystal field parameter is an ingredient of ligand field multiplet (LFM) calculations and is usually taken from optical spectroscopy (Arrio et al, 2000). In order to fit the Fe *K* pre-edge of high spin Fe^{3+} in O_h symmetry (in andradite) using LFM calculations, Arrio et al (2000) used a Δ_0 value of 1.5 eV, which is identical to the P_1-P_2 energy separation determined in this work. Our Δ_0 value is lower than the 1.9 eV deduced from a fitting procedure of diffuse reflectance spectra of goethite and aluminous goethite (Sherman and Waite, 1985; Scheinost et al, 1999). Scheinost et al (1999) show that Δ_0 increases linearly with the Al concentration but this increase is too weak (0.06 eV) to be observable in XANES pre-edge spectra.

Experimental spectra exhibit an intensity decrease of the pre-edge with increasing Al concentration (inset of Fig. 2a). The two energetically favourable models reproduce properly this trend. For the 25 mol % cluster model, the pre-edge features are less intense than for the 8.3 mol % isolated models. This is explained by a smaller number of Fe cation neighbours around Al* (Table 1). This pre-edge analysis supports a distribution of Al atoms that tends to be clustered as the Al concentration increases.

4.3 Validity of the structural models

As shown before, energetic considerations allow to rule out the 25 mol % isolated model and suggest a preferential isolated distribution of Al at 8.3 mol %. These conclusions are not in total agreement with the results of Bazilevskaya et al (2011), which favour the cluster models at both concentrations. Our structural models are built using the same $1 \times 3 \times 2$ supercell and the same atomic configurations as those studied by Bazilevskaya et al (2011), however, our calculated unit cell volumes are significantly different. In the present study, the calculated volumes do not differ much (< 0.26 Å^3) between the cluster and isolated configurations for both concentrations (Table 1). In contrast, Bazilevskaya et al (2011) observed volume variations greater than 14 Å^3. Moreover our theoretical volumes decrease as the Al concentration increases, whereas the opposite trend is observed for the cluster configurations obtained by Bazilevskaya et al (2011). Experimentally, even if a small deviation of the *a* cell parameter from the Vegard's law is observed, it has been shown that the volume of the unit cell decreases with increasing Al concentration [see Blanchard et al (2014) and references therein]. The experimental difference between the volume at 8.3 and 25 mol % is 3.5 Å^3 (Table 1) and the present study displays a calculated value of 3.1 Å^3 in good agreement with 3.5 Å^3, for

the most stable configurations.

To summarize, based on both XANES study and total energy calculations, the cluster arrangement is clearly preferred at high Al concentration. This result supports the assumption of Ildefonse et al (1998), upon which Al could be distributed with AlO_6 sharing both edges and corners (as in diaspore). At low Al concentration, the isolated and cluster configurations energetically differ by 33 meV, but cannot be distinguished by the XANES theoretical-experimental combined study. Therefore, at low Al concentration, the assumption of Ildefonse et al (1998) upon which Al is distributed with edge-sharing AlO_6 octahedra (as in the gibbsite structure) is not verified.

5 Conclusion

The local environment of Al in aluminous goethite is studied through Al *K*-edge XANES spectra measurements and modelling. Three main spectral changes are observed in experimental XANES spectra along the partial solid solution goethite-diaspore. First, the A-B peak spacing is larger in diaspore than in aluminous goethite. Second, the intensities of the A and B peaks decrease, as well as the B/A ratio, when the Al concentration increases. Finally, the intensities of the pre-edge peaks P_1 and P_2 also decrease with increasing Al concentration. These experimental trends are successfully reproduced by the DFT calculations. At low concentrations (i.e., 8.3 mol %), the isolated distribution is likely more favourable than the cluster one while at higher concentrations (i.e., 25 mol %) the cluster arrangement should be considered over the isolated one. The theoretical investigation allows us to identify the structural and electronic parameters controling the spectral evolutions. The nature of cations around the Al impurities impact the A-B peak spacing, which increases when the number of Al neighbours increases. The decrease in Al-Fe(Al) bond length and the distortion of the coordination octahedra explain the decrease of the B/A intensity ratio. In a clustered arrangement of Al, the number of Fe atoms around the Al* absorber decrease (and consequently, the available empty t_{2g} and e_g *d* states), which accounts for the intensity decrease in the pre-edge region. Empty 3*d* orbitals of Fe surrounding Al* are thus indirectly probed through Al *K*-edge XANES measurements. Therefore the Al *K* pre-edge region provides an experimental value of the crystal field splitting of high spin Fe^{3+} 3*d* states in aluminous goethite, in complete agreement with DFT calculations.

Acknowledgements

We acknowledge SOLEIL for provision of synchrotron radiation facilities on the LUCIA beamline (project n°: 99140120). This work was performed using HPC resources from GENCI-IDRIS (Grant 2014 - 100172). This work has been supported by the French National Research Agency (ANR, project 11-JS56-001 "CrIMin"). The authors thank Blair Lebert for proofreading the manuscript. Etienne Balan and Amélie Juhin are acknowledged for fruitful discussions. DC dedicates this paper to the memory of her late colleague, Philippe Ildefonse.

References

Alvarez M, Rueda EH, Sileo E (2007) Simultaneous incorporation of Mn and Al in the goethite structure. Geochim Cosmochim Acta 71:1009–1020

Arrio MA, Rossano S, Brouder C, Galoisy L, Calas G (2000) Calculation of multipole transitions at the Fe *K* pre-edge through $p-d$ hybridization in the Ligand Field Multiplet model. Europhys Lett 51:454–460

Bazilevskaya E, Archibald D, Aryanpour M, Kubicki J, Martínez C (2011) Aluminum coprecipitates with Fe (hydr)oxides: Does isomorphous substitution of Al^{3+} for Fe^{3+} in goethite occur? Geochim Cosmochim Acta 75:4667–4683

Blanch AJ, Quinton JS, Lenehan CE, Pring A (2008) The crystal chemistry of Al-bearing goethites: an infrared spectroscopic study. Mineral Mag 72:1043–1056

Blanchard M, Balan E, Giura P, Béneut K, Yi H, Morin G, Pinilla C, Lazzeri M, Floris A (2014) Infrared spectroscopic properties of goethite: anharmonic broadening, long-range electrostatic effects and Al substitution. Phys Chem Miner 41:289–302

Brouder C, Cabaret D, Juhin A, Sainctavit P (2010) Effect of atomic vibrations on the x-ray absorption spectra at the *K* edge of Al in α-Al_2O_3 and of Ti in TiO_2 rutile. Phys Rev B 81:115,125

Cabaret D, Brouder C (2009) Origin of the pre-edge structure at the Al *K*-edge: The role of atomic vibrations. J Phys Conf Ser 190:012,003

Cabaret D, Gaudry E, Taillefumier M, Sainctavit P, Mauri F (2005) XANES calculation with an efficient "non muffin-tin" method: application to the angular dependence of the Al K-edge in corundum. Phys Scr T115:131–133

Cornell R, Schwertmann U (2003) The iron oxides: structure, properties, reactions, occurrences and uses. Wiley-VCH, Weinheim

de Groot F, Grioni M, Fuggle J, Ghijsen J, Sawatzky G, Petersen H (1989) Oxygen 1*s* x-ray-absorption edges of transition-metal oxides. Phys Rev B 40:5715–5723

Farnan I, Balan E, Pickard C, Mauri F (2003) The effect of radiation damage on local structure in crystalline $ZrSiO_4$: Investigating the ^{29}Si NMR response to pressure in zircon and reidite. Am Mineral 88:1663–1668

Flank AM, Cauchon G, Lagarde P, Bac S, Janousch M, Wetter R, Dubuisson JM, Idir M, Langlois F, Moreno T, Vantelon D (2006) LUCIA, a microfocus soft XAS beamline. Nucl Instrum Methods Phys Res B 246:269–274

Fleet M (1976) Distortion parameters for coordination polyhedra. Mineral Mag 40:531–533

Fleisch J, Grimm R, Gruübler J, Gütlich P (1980) Determination of the aluminum content of natural and synthetic alumogoethites using Mössbauer spectroscopy. J Phys 41:C1–169

Fritsch E, Morin G, Bedidi A, Bonnin D, Balan E, Caquineau S, Calas G (2005) Transformation of haematite and Al-poor goethite to Al-rich goethite and associated yellowing in a ferralitic clay soil profile of the middle Amazon Basin (Manaus, Brazil). Eur J Soil Sci 56:575–588

Garrity K, Bennett J, Rabe K, Vanderbilt D (2014) Pseudopotentials for high-throughput DFT calculations. Comput Mater Sci 81:446–452

Gaudry E, Cabaret D, Sainctavit P, Brouder C, Mauri F, Goulon J, Rogalev A (2005) Structural relaxations around Ti, Cr and Fe impurities in α-Al_2O_3 probed by x-ray absorption near edge structure combined with first-principles calculations. J Phys Condens Matter 17:5467–5480

Gaudry E, Cabaret D, Brouder C, Letard I, Rogalev A, Wilhlem F, Jaouen N, Sainctavit P (2007) Relaxations around the substitutional chromium site in emerald: X-ray absorption experiments and density functional calculations. Phys Rev B 76:094,110

Giannozzi P, Baroni S, Bonini N, Calandra M, Car R, Cavazzoni C, Ceresoli D, Chiarotti GL, Cococcioni M, Dabo I, Dal Corso A, de Gironcoli S, Fabris S, Fratesi G, Gebauer R, Gerstmann U, Gougoussis C, Kokalj A, Lazzeri M, Martin-Samos L, Marzari N, Mauri F, Mazzarello R, Paolini S, Pasquarello A, Paulatto L, Sbraccia C, Scandolo S, Sclauzero G, Seitsonen AP, Smogunov A, Umari P, Wentzcovitch RM (2009) QUANTUM ESPRESSO: a modular and open-source software project for quantum simulations of materials. J Phys Condens Matter 21:395,502

Gilbert B, Kim CK, Dong CL, Guo J, Nico PS, Shuh DK (2007) Oxygen K-edge emission and absorption spectroscopy in iron oxyhydroxide nanoparticles. AIP Conf Proc 882:721–725, proc. of the XAFS-13 conference, Stanford, USA, July 2006

Goodman B, Lewis D (1981) Mössbauer spectra of aluminous goethites. J Soil Sci 32:351–364

Gougoussis C, Calandra M, Seitsonen A, Mauri F (2009) First-principles calculations of x-ray absorption in a scheme based on ultrasoft pseudopotentials: From α-quartz to high-Tc compounds. Phys Rev B 80:075,102

Ildefonse P, Cabaret D, Sainctavit P (1998) Aluminium X-ray absorption near edge structure in model compounds and Earth's surface minerals. Phys Chem Miner 25:112–121

Kas JJ, Sorini AP, Prange MP, Cambell LW, Soininen JA, Rehr JJ (2007) Many-pole model of inelastic losses in x-ray absorption spectra. Phys Rev B 76:195,116

Kas JJ, Vinson J, Trcera N, Cabaret D, Shirley EL, Rehr JJ (2009) Many-pole model of inelastic losses applied to calculations of XANES. J Phys Conf Ser 190:012,009, proc. of the XAFS-14 conference, Camerino, Italie, July 2009

Kaur N, Gräfe M, Singh B, Kennedy B (2009) Simultaneous incorporation of Cr, Zn, Cd, and Pb in the goethite structure. Clays Clay Miner 57:234–250

Kim J, Ilott AJ, Middlemiss DS, Chernova NA, Pinney N, Morgan D, Grey CP (2015) ^{2}H and ^{27}Al solid-state NMR study of the local environments in Al-doped 2-line ferrihydrite, goethite, and lepidocrocite. Chem Mater 27:3966–3978

König E, Kremer S (1977) Ligand field energy diagrams. Plenum Publishing Corporation

Lelong G, Radtke G, Cormier L, Bricha H, Rueff JP, Ablett JM, Cabaret D, GÃl'lÃl'bart F, Shukla A (2014) Detecting non-bridging oxygens: Non-resonant inelastic x-ray scattering in crystalline lithium borates. Inorg Chem 53:10,903–10,908

Liu Q, Yu Y, Torrent J, Roberts A, Pan Y, Zhu R (2006) Characteristic low-temperature magnetic properties of aluminous goethite [α -(Fe, Al)OOH] explained. J Geophys Res 111:B12S34

Manuel D, Cabaret D, Brouder C, Sainctavit P, Bordage A, Trcera N (2012) Experimental evidence of thermal fluctuations on the x-ray absorption near-edge structure at the aluminum *K* edge. Phys Rev B 85:224,108

Mitchell MR, Reader SW, Johnston KE, Pickard CJ, Whittle KR, Ashbrook SE (2011) ^{119}Sn MAS NMR and first-principles calculations for the investigation of disorder in stannate pyrochlores. Phys Chem Chem Phys 13:488–497

Monkhorst H, Pack J (1976) Special points for Brillouin-zone integrations. Phys Rev B 13:1227–1230

Murad E, Schwertmann U (1983) The influence of aluminum substitution and crystallinity on the Mössbauer-spectra of goethite. Clay Miner 18:301–312

Otte K, Pentcheva R, Schmahl WW, Rustad J (2009) Pressure-induced structural and electronic transitions in FeOOH from first principles. Phys Rev B 80:205,116

Perdew JP, Burke K, Ernzerhof M (1996) Generalized Gradient Approximation Made Simple. Phys Rev Lett 77:3865–3868

Robinson K, Gibbs GV, Ribbe PH (1971) Quadratic elongation: A quantitative measure of distortion in coordination polyhedra. Sci 172:567–570

Russell B, Payne M, Ciacchi L (2009) Density functional theory study of Fe(II) adsorption and oxidation on goethite surfaces. Phys Rev B 79:165,101

Scheinost A, Schulze DG, Schwertmann U (1999) Diffuse reflectance spectra of Al substituted goethite: a ligand field approach. Clays Clay Miner 47:156–164

Schulze DG (1984) The influence of aluminum on iron oxides. VIII. Unit-cell dimensions of Al-substitued goethites and estimation of Al from them. Clays Clay Miner 32:36–44

Schulze DG, Schwertmann U (1987) The influence of aluminium on iron oxides: XII. Properties of goethites synthesised in 0·3 M KOH at 25°C. Clay Miner 22:83–92

Schwertmann U (1984) The influence of aluminium on iron oxides: IX. Dissolution of Al-goethites in 6 M HCl. Clays Miner 19:9–19

Sherman D, Waite T (1985) Electronic spectra of Fe^{3+} oxides and oxide hydroxides in the near IR to near UV. Am Mineral 70:1262–1269

Taillefumier M, Cabaret D, Flank AM, Mauri F (2002) X-ray absorption near-edge structure calculations with the pseudopotentials: Application to the K edge in diamond and α-quartz. Phys Rev B 66(19):195,107

Trcera N, Cabaret D, Rossano S, Farges F, Flank AM, Lagarde P (2009) Experimental and theoretical study of the structural environment of magnesium in minerals and silicate glasses using x-ray absorption near-edge structure. Phys Chem Miner 36:241–257

Trivedi P, Axe L, Dyer J (2001) Adsorption of metal ions onto goethite: single-adsorbate and competitive systems. Colloids Surf, A 191:107–121

Wang S, Mao W, Sorini A, Chen CC, Devereaux T, Ding Y, Xiao Y, Chow P, Hiraoka N, Ishii H, Cai Y, Kao CC (2010) High-pressure evolution of Fe_2O_3 electronic structure revealed by x-ray absorption. Phys Rev B 82:144,428

Wells MA, Fitzpatrick R, Gilkes R (2006) Thermal and mineral properties of Al-, Cr-, Mn-, Ni- and Ti-substituted goethite. Clays Clay Miner 54:176–194

Zhang J, Wu Z, Ibrahim K, Abbas M, Ju X (2003) Surface structure of α-Fe2O3 nanocrystal observed by O *K*-edge X-ray absorption spectroscopy. Nucl Instrum Methods Phys Res B 199:291–294